npg

ORIGINAL ARTICLE

Beneficial effects of selective HDL-raising gene transfer on survival, cardiac remodelling and cardiac function after myocardial infarction in mice

SC Gordts, I Muthuramu, E Nefyodova, F Jacobs, E Van Craeyveld and B De Geest

Post-myocardial infarction (MI) ejection fraction is decreased in patients with low high-density lipoprotein (HDL) cholesterol levels, independent of the degree of coronary atherosclerosis. The objective of this study is to evaluate whether selective HDL-raising gene transfer exerts cardioprotective effects post MI. Gene transfer in C57BL/6 low-density lipoprotein receptor (LDLr)$^{-/-}$ mice was performed with the E1E3E4-deleted adenoviral vector AdA-I, inducing hepatocyte-specific expression of human apo A-I, or with the control vector Adnull. A ligation of the left anterior descending coronary artery was performed 2 weeks after transfer or saline injection. HDL cholesterol levels were persistently 1.5-times ($P < 0.0001$) higher in AdA-I mice compared with controls. Survival was increased ($P < 0.01$) in AdA-I MI mice compared with control MI mice during the 28-day follow-up period (hazard ratio for mortality 0.42; 95% confidence interval 0.24–0.76). Longitudinal morphometric analysis demonstrated attenuated infarct expansion and inhibition of left ventricular (LV) dilatation in AdA-I MI mice compared with controls. AdA-I transfer exerted immunomodulatory effects and increased neovascularisation in the infarct zone. Increased HDL after AdA-I transfer significantly improved systolic and diastolic cardiac function post MI, and led to a preservation of peripheral blood pressure. In conclusion, selective HDL-raising gene transfer may impede the development of heart failure.

INTRODUCTION

High-density lipoprotein (HDL) cholesterol levels are inversely correlated with the incidence of ischaemic cardiovascular diseases.[1] This inverse relationship is attributed to the role of HDL in reverse cholesterol transport, but may also be related to its antioxidative, anti-inflammatory, anti-apoptotic and endothelial protective features.[2,3] These pleiotropic properties offer an interesting perspective to evaluate the therapeutic potential of HDL outside the classical field of atherosclerosis. Apolipoprotein (apo) A-I is the main apo of HDL and apo A-I levels strongly correlate with HDL cholesterol concentrations. Human *apo A-I* gene transfer has been shown to selectively increase HDL.[4–6]

Post-infarct ejection fraction is lower in patients with low HDL cholesterol levels.[7,8] The Framingham Heart Study demonstrated an enduring relation between low HDL cholesterol and heart failure incidence after exclusion of baseline coronary heart disease and accounting for interim myocardial infarction (MI).[9] Moreover, low HDL cholesterol levels and low levels of apo A-I indicate an unfavourable prognosis in patients with heart failure, independent of the aetiology.[10,11]

Direct cellular effects of HDL have been demonstrated in isolated cardiomyocytes *in vitro*, as evidenced by increased phosphorylation of extracellular signal-regulated kinases 1/2,[12] of the transcription factor signal transducer and activator of transcription 3[12] and of the pro-survival kinase Akt.[13] Furthermore, Van Linthout *et al.*[13] have previously shown that HDL inhibits cardiomyocyte apoptosis under conditions of hyperglycaemia.

Finally, the development of diabetic cardiomyopathy is inhibited by human *apo A-I* gene transfer in rats.[13]

Taken together, epidemiological and experimental studies provide converging lines of evidence that HDL may exert direct protective effects on the myocardium. Whereas no selective HDL-raising drugs are currently available in the clinic, hepatocyte-directed human *apo A-I* gene transfer is an experimental HDL-targeted intervention. The goal of this study is, therefore, to investigate whether selective HDL-raising human *apo A-I* gene transfer exerts beneficial effects on cardiac remodelling and on cardiac function following MI. We show that human *apo A-I* gene transfer in C57BL/6 low-density lipoprotein receptor (LDLr)-deficient mice increases survival, decreases infarct expansion, attenuates left ventricular (LV) dilatation and improves cardiac function, following permanent ligation of the left anterior descending coronary artery (LAD).

RESULTS

Human *apo A-I* gene transfer selectively increases HDL in C57BL/6 LDLr$^{-/-}$ mice

C57BL/6 LDLr$^{-/-}$ mice were fed a diet containing 0.2% (w/w) cholesterol and 10% (v/v) coconut oil starting at the age of 12 weeks. Three weeks after the start of the diet, the mice were treated with the E1E3E4-deleted adenoviral human apo A-I-expressing vector AdA-I. Control mice were injected with the control vector Adnull or with saline buffer. Neither Adnull gene

Centre for Molecular and Vascular Biology, Department of Cardiovascular Sciences, Catholic University of Leuven, Leuven, Belgium. Correspondence: Professor B De Geest, Centre for Molecular and Vascular Biology, Department of Cardiovascular Sciences, Catholic University of Leuven, Campus Gasthuisberg Herestraat 49 bus 911, Leuven, Vlaams Brabant 3000, Belgium.
E-mail: bart.degeest@med.kuleuven.be

Table 1. Lipoprotein cholesterol levels on day 10 and day 42 after saline injection or gene transfer in C57BL/6 LDLr $^{-/-}$ mice

	Controls (n = 8)		AdA-I (n = 8)	
	Day 10	Day 42	Day 10	Day 42
VLDL cholesterol (mg dl^{-1})	80.5 ± 3.2	78.4 ± 4.3	76.6 ± 3.5	76.2 ± 5.1
IDL cholesterol (mg dl^{-1})	166 ± 12	169 ± 7	156 ± 11	162 ± 10
LDL cholesterol (mg dl^{-1})	157 ± 12	161 ± 10	159 ± 8	158 ± 12
HDL cholesterol (mg dl^{-1})	72.3 ± 3.5	69.7 ± 4.1	108 ± 4****	106 ± 4****
Non-HDL cholesterol (mg dl^{-1})	403 ± 16	409 ± 11	392 ± 11	397 ± 13
Total cholesterol (mg dl^{-1})	476 ± 13	478 ± 8	500 ± 13	503 ± 12

Abbreviations: HDL, high-density lipoprotein; IDL, intermediate-density lipoprotein; LDL, low-density lipoprotein; LDLr, low-density lipoprotein receptor; VLDL, very-low-density lipoprotein. Control mice were injected with Adnull (n = 4) or saline (n = 4). Data are expressed as means ± s.e.m. ****$P < 0.0001$ versus controls.

transfer nor saline injection was shown to alter cholesterol levels compared with pre-injection values, and the data of both control groups were pooled. Gene transfer with the E1E3E4-deleted human apo A-I-expressing vector AdA-I induced human apo A-I levels of 220 ± 27 mg dl^{-1} (n = 8) and 208 ± 36 mg dl^{-1} (n = 8) on days 10 and 42, respectively, after injection. This resulted in a 1.5-fold ($P < 0.0001$) increase of HDL cholesterol on days 10 and 42 after injection, compared with controls (Table 1). No significant alteration of very-low-density lipoprotein cholesterol, intermediate-density lipoprotein cholesterol and LDL cholesterol was observed after AdA-I transfer, compared with the control mice (Table 1).

Increased HDL following AdA-I transfer improves survival after MI in C57BL/6 LDLr$^{-/-}$ mice

MI was induced 2 weeks after gene transfer or saline injection by permanent ligation of the LAD. Comparison of Kaplan–Meier survival curves (Figure 1) showed a lower mortality rate in AdA-I-treated MI mice compared with the control MI mice ($P < 0.01$) (hazard ratio for mortality 0.42, 95% confidence interval 0.24–0.76). Autopsy data revealed that ventricular rupture was the cause of death in all but one mouse, indicating that AdA-I transfer significantly reduced the occurrence of ventricular rupture. To test whether the enhanced survival in AdA-I MI mice may be related to immunomodulatory effects of HDL and to accelerated infarct scar development, interleukin (IL)10, IL1β, transforming growth factor β1, collagen type I α1 and collagen type III α1 mRNA levels were quantified in the infarct zone on day 3. Data in Supplementary Table 1 illustrate that AdA-I gene transfer resulted in immuno-modulatory and profibrogenic effects in the infarct zone.

Human apo A-I gene transfer reduces infarct expansion

Infarct area and total area at risk were determined at 24 h after ligation of the LAD in control mice and AdA-I mice to exclude a potential difference in myocardial necrosis (Table 2). The total area at risk and the infarct area were not significantly different at 24 h after ligation of the LAD in control and AdA-I-treated mice. In addition, the LV cavity area and the LV wall area were similar at 24 h in both groups (data not shown).

The time course of infarct length and infarct thickness is illustrated in Figures 2a and b, respectively. Figure 2a shows that a significant increase of infarct length occurred in both the control MI mice and the AdA-I MI mice between days 3 and 14. However, infarct length on day 28 was 24% ($P < 0.05$) shorter in AdA-I MI mice than in control MI mice. Attenuated infarct expansion in AdA-I MI mice was also evidenced by a 41% ($P < 0.001$) increase in the infarct thickness (Figure 2b) on day 28 compared with the control MI mice. Taken together, these results show that AdA-I transfer profoundly mitigates infarct expansion. The delayed divergence of both the infarct length and infarct thickness curves may be explained by the observed difference in mortality in the
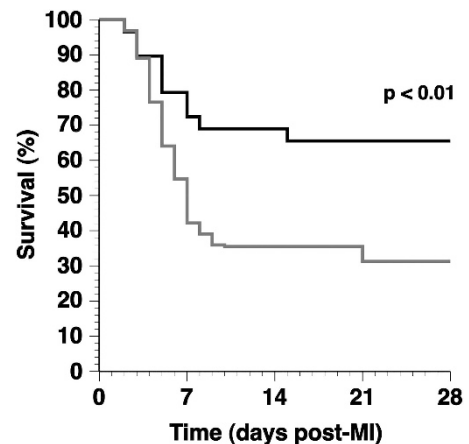
Figure 1. Kaplan–Meier survival curves after MI in control mice and in AdA-I-treated mice during the 28-day follow-up period. At the start of the study, 64 control MI mice (grey) and 29 AdA-I MI mice (black) were included. Survival analysis was performed by log-rank test.

first 2 weeks (Figure 1), which eliminates MI mice with the most pronounced infarct expansion and consequent cardiac rupture.

Improved infarct healing at the histological level was evidenced by an increase of collagen content on day 28 in the infarct zone of AdA-I MI mice (40.8 ± 1.6%) compared with the control MI mice (37.0 ± 1.5%) ($P = 0.057$). Furthermore, capillary density was 36% ($P < 0.05$) higher on day 28 in the infarct zone of AdA-I MI mice than in the control MI mice (Table 3). To evaluate whether enhanced endothelial progenitor cell (EPC) incorporation contributed to increased capillary density in the infarct zone of AdA-I MI mice, transplantations with bone marrow of C57BL/6 β-actin green-fluorescent protein (GFP) mice were performed 4 weeks before the start of the diet. The peripheral blood count in mice 6 weeks after bone marrow transplantation was similar compared with mice without bone marrow transplantation (data not shown). The density of GFP-positive capillaries was not significantly different between chimeric control MI mice and AdA-I MI mice (Table 3), indicating a similar degree of incorporation of bone marrow-derived EPCs.

Increased HDL following AdA-I transfer attenuates LV dilatation after MI

LV cavity area and LV muscle area were determined on day 0 before MI, and on days 3, 14 and 28 after MI (Figure 3). The LV cavity area increased 3.8-fold ($P < 0.001$) between days 0 and 28 in control MI mice and was 38% ($P < 0.05$) larger compared with AdA-I MI mice on day 28 (Figure 3a). The delayed divergence of

both curves should be interpreted in light of the survival bias. LV muscle area was 44% ($P < 0.01$) and 49% ($P < 0.01$) lower on day 3, compared with day 0 in control MI and AdA-I MI mice, respectively (Figure 3b). This decrease is consistent with data on infarct area on day 1 (Table 2). The subsequent increase of LV muscle area between days 3 and 28 (Figure 3b), consistent with LV hypertrophy, was not significantly different between both groups. Cardiomyocyte hypertrophy was evidenced by a 96% ($P < 0.001$) and 81% ($P < 0.001$) increase of cardiomyocyte cross-sectional area between days 0 and 28 in control MI and AdA-I MI mice, respectively (Figure 3c). This was associated with a reduction of capillary density on day 28 by 37% ($P < 0.001$) and by 23% ($P < 0.001$) in control MI and AdA-I MI mice, respectively,

compared with day 0 (Figure 3d). Representative laminin stainings of the myocardium illustrating development of cardiomyocyte hypertrophy in control MI mice are illustrated in Figure 4.

Data on interstitial fibrosis on day 28 after MI are summarised in Supplementary Table 2. Immature collagen was 28% ($P < 0.05$) lower in AdA-I MI mice compared with the control MI mice, whereas no significant difference in the amount of mature collagen in the interstitium was observed.

Human apo A-I gene transfer improves cardiac function after MI

Hemodynamic parameters in the left ventricle and in the aorta on day 28 in control MI mice and AdA-I MI mice in comparison with reference values in sham C57BL/6 LDLr$^{-/-}$ mice are shown in Table 4. The LV peak systolic pressure was significantly higher in AdA-I MI mice than in control MI mice ($P < 0.05$). The mean peripheral blood pressure ($P < 0.01$), systolic peripheral blood pressure ($P < 0.01$) and diastolic peripheral blood pressure ($P < 0.05$) were significantly higher in AdA-I MI mice compared with the control MI mice. Compared to reference control mice, blood pressure was preserved in AdA-I MI mice, but was significantly lower in control MI mice (Table 4). The increased peak rate of isovolumetric contraction (dP/dt max; $P < 0.01$) in AdA-I MI mice compared with control MI mice points to an improvement of systolic function. The higher peak rate of isovolumetric relaxation (dP/dt min; $P < 0.01$) and the lower time constant of LV relaxation (τ) ($P < 0.05$) are indicative of an improved diastolic function in AdA-I MI mice compared with control MI mice. Taken together, AdA-I gene transfer beneficially affected systolic and diastolic cardiac

Table 2. Infarct area and area at risk 24 h after permanent ligation of the LAD

	Control MI n = 6	AdA-I MI n = 5
Total area at risk (% of left ventricular wall area)	49.0 ± 2.2	54.1 ± 3.9
Infarct area (% of left ventricular wall area)	48.4 ± 2.2	53.0 ± 3.7
Non-infarcted area at risk (% of left ventricular wall area)	0.600 ± 0.200	1.09 ± 0.37
Infarct area (% of total area at risk)	98.8 ± 0.5	98.1 ± 0.6

Abbreviations: LAD, left anterior descending coronary artery; MI, myocardial infarction. Data are expressed as means ± s.e.m.
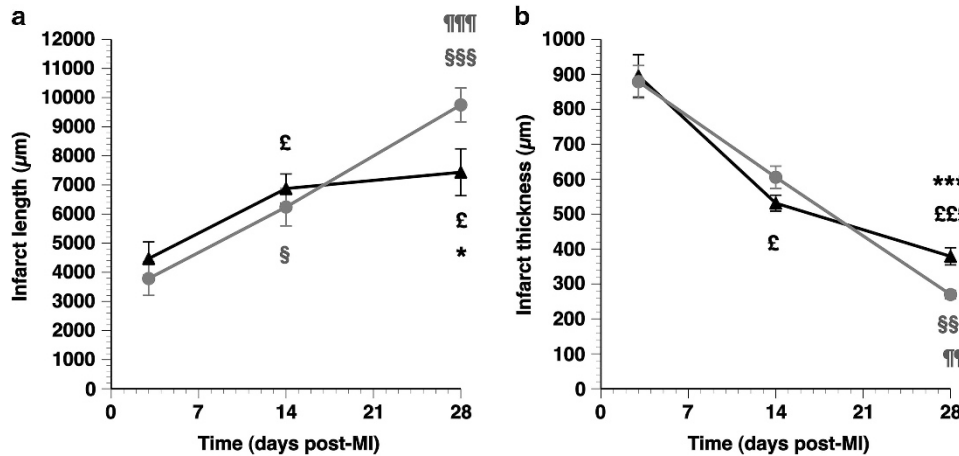

Figure 2. Time course of infarct length (a) and infarct thickness (b) in control MI mice (grey circles) and AdA-I MI mice (black triangles). Morphometric analyses were performed on day 3 ($n = 9$ for control, $n = 11$ for AdA-I), day 14 ($n = 10$ for controls, $n = 9$ for AdA-I) and day 28 after MI ($n = 16$ in both groups). Data represent means ± s.e.m. §$P < 0.05$; §§§$P < 0.001$ for longitudinal comparisons versus day 3 control MI. ₤$P < 0.05$; ₤₤₤$P < 0.001$ for longitudinal comparisons versus day 3 AdA-I MI. ¶¶$P < 0.01$; ¶¶¶$P < 0.001$ for comparison between day 14 and day 28 control MIs. *$P < 0.05$; ***$P < 0.001$ for control MI versus AdA-I MI.

Table 3. Quantification of total capillaries and capillaries containing bone marrow-derived GFP-positive-incorporated EPCs in the infarct zone

	No prior bone marrow transplantation		Prior bone marrow transplantation	
	Control MI (n = 16)	AdA-I MI (n = 16)	Control MI (n = 16)	AdA-I MI (n = 14)
Capillary density (number mm^{-2})	145 ± 16	197 ± 19*	144 ± 14	198 ± 21*
GFP-positive capillary density (number mm^{-2})	N.A.	N.A.	30.7 ± 8.0	35.9 ± 8.6
GFP-positive capillaries (% of total capillaries)	N.A.	N.A.	19.3 ± 4.2	18.0 ± 3.4

Abbreviations: EPC, endothelial progenitor cell; GFP, green-fluorescent protein; MI, myocardial infarction; N.A., not applicable. Data are expressed as means ± s.e.m. *$P < 0.05$ for control MI versus AdA-I MI.
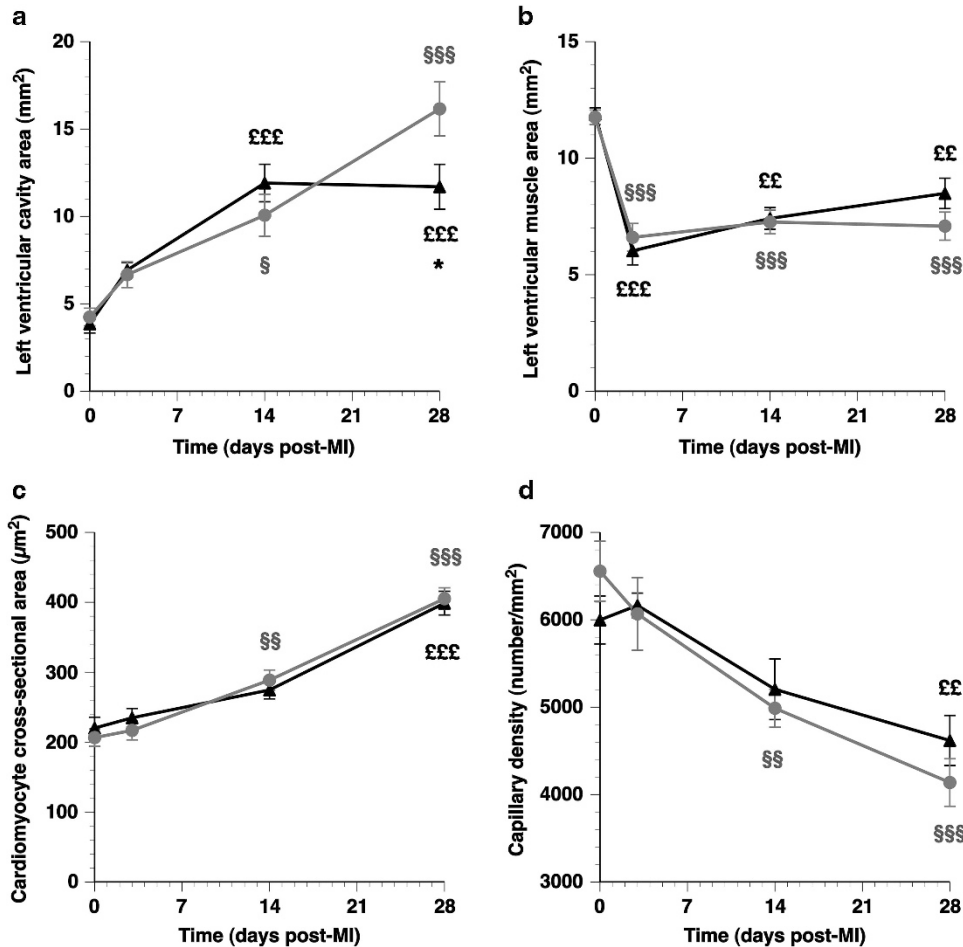
Figure 3. Time course of left ventricular remodelling in control MI mice (grey circles) and AdA-I MI mice (black triangles). Longitudinal changes in left ventricular cavity area, left ventricular muscle area, cardiomyocyte cross-sectional area and capillary density are illustrated in panels (**a–d**), respectively. Data represent means ± s.e.m. (n is identical as indicated in the Legend to Figure 2). For reasons of clarity, only statistical differences between day 0 and other time points, or differences between control MI mice and AdA-I MI mice are indicated. [§]$P < 0.05$; [§§]$P < 0.01$; [§§§]$P < 0.001$ for longitudinal comparisons versus day 0 control MI. [££]$P < 0.01$; [£££]$P < 0.001$ for longitudinal comparisons versus day 0 AdA-I MI. [*]$P < 0.05$ for control MI versus AdA-I MI.
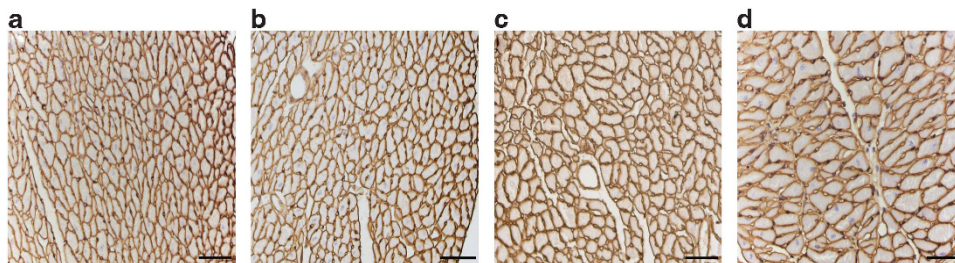
Figure 4. Representative laminin stainings of myocardial tissue illustrating development of cardiomyocyte hypertrophy in control MI mice. Representative photomicrographs show laminin-stained cardiomyocytes on day 0 (panel **a**), day 3 (panel **b**), day 14 (panel **c**) and day 28 (panel **d**) after MI. Scale bar represents 500 μm.

function after MI, and induced a preservation of blood pressure compared with the sham control mice.

Prior irradiation and bone marrow transplantation enhance survival and attenuate LV dilatation in control MI mice, but beneficial effects of AdA-I transfer on cardiac structure and cardiac function remain

In the experiments designed to evaluate EPC incorporation, we made the startling observation that prior irradiation and bone

marrow transplantation significantly reduced mortality in control MI mice ($P < 0.0001$) (hazard ratio for mortality 0.23, 95% confidence interval 0.12–0.46) (Figure 5a) and in AdA-I MI mice ($P < 0.05$) (hazard ratio for mortality 0.28, 95% confidence interval 0.081–0.96) (Figure 5b) compared with the respective MI groups without prior bone marrow transplantation. Table 5 summarises infarct parameters and remodelling parameters on day 28 in control MI mice and AdA-I MI mice without and with prior bone marrow transplantation. Infarct area and infarct length were

Table 4. Hemodynamic parameters in the left ventricle and in the aorta on day 28 after myocardial infarction in comparison with reference values in sham C57BL/6 LDLr$^{-/-}$ mice

	Sham (n = 19)	Control MI (n = 11)	AdA-I MI (n = 11)
Left ventricle			
Peak systolic pressure (mm Hg)	103 ± 2	84.9 ± 2.6§§§	95.9 ± 3.8*
End-diastolic pressure (mm Hg)	2.19 ± 0.68	4.81 ± 1.75	1.92 ± 0.92
Peak dP/dt max (mm Hg ms^{-1})	12.1 ± 0.6	6.60 ± 0.27§§§	9.01 ± 0.54§§**
Peak dP/dt min (mm Hg ms^{-1})	− 8.7 ± 0.38	− 5.57 ± 0.23§§§	− 7.32 ± 0.48§**
Tau (ms)	5.19 ± 0.29	6.90 ± 0.35§§	5.75 ± 0.31*
Heart rate (bpm)	601 ± 15	554 ± 23	573 ± 26
Aorta			
Mean pressure (mm Hg)	78.8 ± 2.1	64.3 ± 2.6§§	78.4 ± 4.2**
Peak systolic pressure (mm Hg)	99.5 ± 2.0	81.0 ± 2.3§§§	96.1 ± 4.4**
Peak diastolic pressure (mm Hg)	60.2 ± 2.7	50.6 ± 3.3	63.2 ± 3.5*

Abbreviations: LDLr, low-density lipoprotein receptor; MI, myocardial infarction. Data are expressed as means ± s.e.m. $^{*}P<0.05$; $^{**}P<0.01$ for comparison versus control MI. $^{§}P<0.05$; $^{§§}P<0.01$; $^{§§§}P<0.001$ versus Sham.
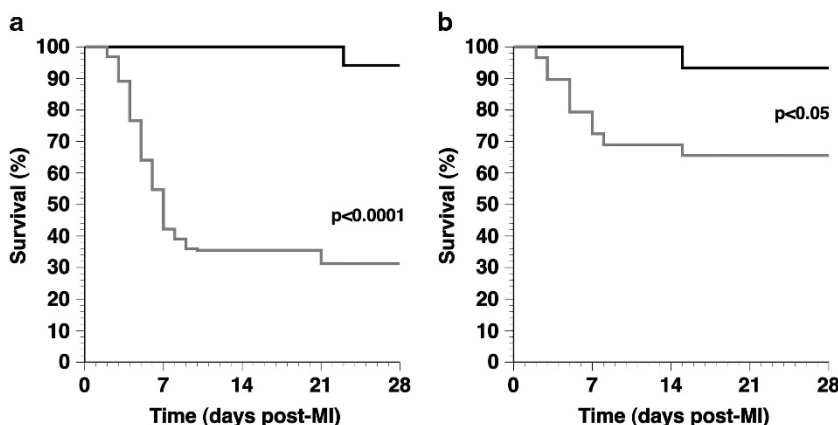
Figure 5. Comparison Kaplan–Meier survival curves after myocardial infarction in mice without (grey line) and with (black line) prior bone marrow transplantation during a 28-day follow-up period. Kaplan–Meier survival curves in panel (**a**) concern control MI mice. At the start of the study, 64 control MI mice without prior bone marrow transplantation and 17 control MI mice with prior bone marrow transplantation were included. Data in panel (**b**) are based on inclusion of 29 AdA-I MI mice without prior bone marrow transplantation and 15 AdA-I mice with prior bone marrow transplantation. Survival analysis was performed by log-rank test.

Table 5. Comparison of infarct parameters and of left ventricular remodelling at day 28 after myocardial infarction in mice without and with prior irradiation and bone marrow transplantation

	No prior bone marrow transplantation		Prior bone marrow transplantation	
	Control MI (n = 16)	AdA-I MI (n = 16)	Control MI (n = 16)	AdA-I MI (n = 14)
Infarct area (mm^2)	3.06 ± 0.16	2.84 ± 0.26	2.44 ± 0.17§	2.05 ± 0.17§
Infarct length (μm)	9750 ± 580	7430 ± 800*	5000 ± 280§§§§	4220 ± 250§§*
Infarct thickness (μm)	270 ± 12	379 ± 25***	590 ± 24§§§§	613 ± 17§§§§
Whole left ventricular area (mm^2)	26.3 ± 1.5	23.0 ± 0.9	19.2 ± 0.5§§§	17.5 ± 0.5§§§§*
Left ventricular cavity area (mm^2)	16.2 ± 1.5	11.7 ± 1.3*	7.30 ± 0.58§§§§	5.98 ± 0.40§§§
Left ventricular muscle area (mm^2)	7.08 ± 0.60	8.49 ± 0.65	9.44 ± 0.36§§	9.46 ± 0.32
Septal wall thickness (μm)	1060 ± 30	1240 ± 60	1100 ± 30	1150 ± 40
Cardiomyocyte cross-sectional area (μm^2)	405 ± 16	399 ± 17	293 ± 12§§§§	282 ± 12§§§§
Capillary density (number mm^{-2})	4140 ± 270	4620 ± 290	3380 ± 180§	3550 ± 170§§

Abbreviation: MI, myocardial infarction. Data are expressed as means ± s.e.m. $^{*}P<0.05$; $^{***}P<0.001$ for control MI versus AdA-I MI. $^{§}P<0.05$; $^{§§}P<0.01$; $^{§§§}P<0.001$; $^{§§§§}P<0.0001$ for prior bone marrow transplantation groups versus respective no prior bone marrow transplantation groups.

significantly reduced, and infarct thickness was significantly increased in control MI mice and in AdA-I MI mice with prior irradiation and bone marrow transplantation compared with the respective MI mice groups without prior bone marrow transplantation. Furthermore, pronounced reductions in LV cavity area were observed in mice with prior irradiation and bone marrow transplantation compared with mice without prior bone marrow transplantation. Selective HDL-raising gene transfer
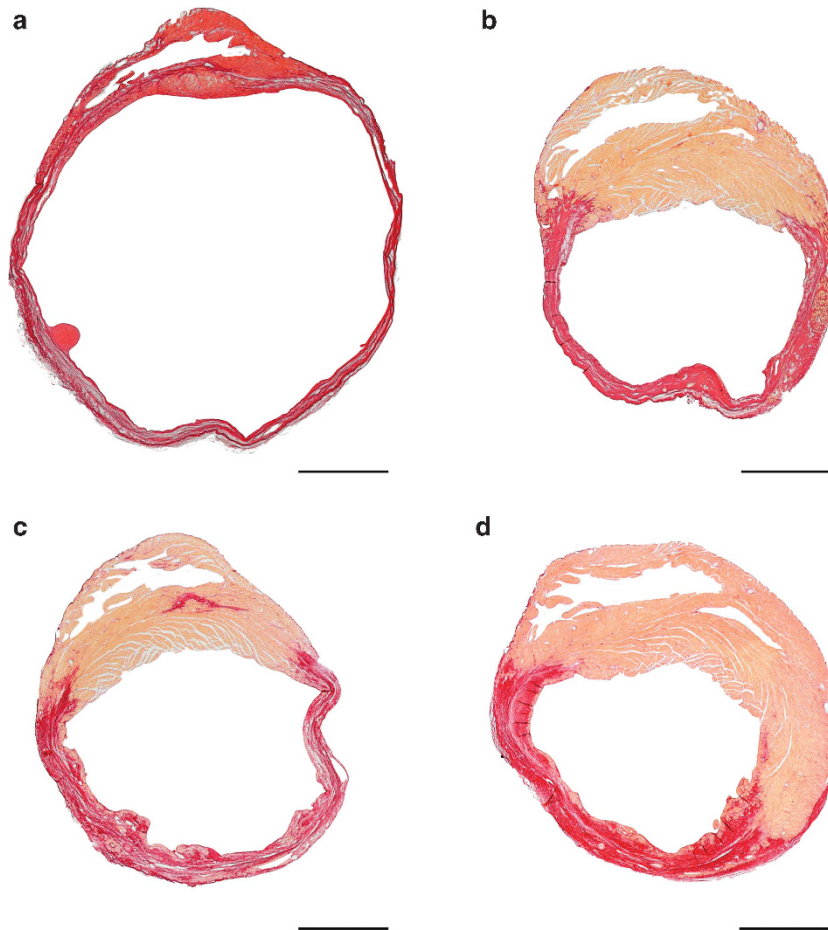
Figure 6. Representative Sirius Red-stained cross-sections of hearts on day 28 after MI in control and AdA-I-treated C57BL/6 LDLr$^{-/-}$ mice without and with prior bone marrow transplantation. Control MI and AdA-I MI mice without prior bone marrow transplantation are illustrated in panel (**a**) and panel (**b**), respectively. Cross-sections of control MI mice and AdA-I MI mice with prior bone marrow transplantation are shown in panel (**c**) and panel (**d**), respectively. Sirius Red stains fibrotic infarct tissue red and healthy tissue orange. Scale bar represents 1 mm.

reduced infarct length by 16% ($P<0.05$) and decreased LV cavity area by 18% ($p=0.079$) in mice with prior irradiation and bone marrow transplantation (Table 5), indicating the robustness of the effects of selective HDL-raising gene transfer on cardiac structure and function. Comparison of representative Sirius Red-stained cross-sections on day 28 after MI in mice without or with prior irradiation and bone marrow transplantation is shown in Figure 6.

Hemodynamic parameters in the left ventricle and in the aorta on day 28 after MI in control MI mice and AdA-I MI mice with prior irradiation and bone marrow transplantation are summarised in Table 6. Similar as in mice without prior bone marrow transplantation, the peak rate of isovolumetric contraction (dP/dt max) was markedly higher in AdA-I MI mice compared with the control MI mice (Table 6). The higher peak rate of isovolumetric relaxation (dP/dt min; $P<0.05$) and the lower time constant of LV relaxation (τ) ($P<0.05$) in AdA-I MI mice with prior bone marrow transplantation than in control MI mice with prior bone marrow transplantation confirm the robustness of the effects of human *apo A-I* gene transfer. In further agreement with hemodynamic data in Table 4, systolic peripheral blood pressure in mice with prior bone marrow transplantation was higher ($P<0.05$) in AdA-I MI mice than in control MI mice (Table 6).

DISCUSSION

The current study shows that hepatocyte-directed human *apo A-I* gene transfer, resulting in a selective increase of HDL, exerts direct

Table 6. Hemodynamic parameters in the left ventricle and the aorta at day 28 after myocardial infarction in bone marrow transplantation C57BL/6 LDLr$^{-/-}$ mice

	Control MI (n = 14)	AdA-I MI (n = 10)
Left ventricle		
Peak systolic pressure (mm Hg)	87.9 ± 3.9	96.7 ± 2.4
End-diastolic pressure (mm Hg)	2.49 ± 1.40	0.565 ± 0.818
dP/dt max (mm Hg ms^{-1})	7.07 ± 0.75	9.90 ± 0.54*
dP/dt min (mm Hg ms^{-1})	− 6.17 ± 0.50	− 7.69 ± 0.39*
Tau (ms)	5.84 ± 0.32	4.93 ± 0.17*
Heart rate (bpm)	577 ± 25	616 ± 21
Aorta		
Mean pressure (mm Hg)	66.9 ± 5.0	75.4 ± 3.2
Systolic pressure (mm Hg)	86.3 ± 4.6	98.4 ± 1.8*
Diastolic pressure (mm Hg)	55.1 ± 5.4	59.1 ± 5.3

Abbreviations: LDLr, low-density lipoprotein receptor; MI, myocardial infarction. Data are expressed as means ± s.e.m. *$P<0.05$ versus control MI.

cardiac effects, leading to improved survival, attenuated infarct expansion, reduced LV dilatation, and enhanced LV systolic and diastolic function post MI. As the objective of this study was to

investigate the effect of HDL on cardiac remodelling and heart failure development, a model of permanent ligation of the LAD was used, which excludes salutary coronary effects of HDL on myocardial salvage, as observed in a model of ischaemia/reperfusion injury.[14] As expected, the infarct area and the area at risk were nearly identical at 24 h after ligation, implying that the initial increase in loading conditions was not different between human *apo A-I* gene transfer MI mice and control MI mice.

Infarct expansion is the disproportionate thinning and dilatation of the infarct segment,[15] and predisposes to myocardial rupture and congestive heart failure.[16–19] The decreased incidence of ventricular rupture in AdA-I MI mice, mainly occurring between days 3 and 14 post MI, can be viewed as a manifestation of attenuated infarct expansion.[20] Our gene expression analysis data in the infarct zone on day 3 indicate that human *apo A-I* gene transfer resulted in immunomodulatory effects, and in accelerated fibrogenesis that may have attenuated infarct expansion and may have reduced the incidence of ventricular rupture. Furthermore, direct effects of apo A-I on the function of monocyte-derived macrophages have been described,[21] which may have contributed to reduced infarct expansion.

Survival bias should be taken into account in the comparison of the morphometric data between days 3 and 14. In contrast, as mortality between days 14 and 28 was very low in both control MI and AdA-I MI mice, the morphometric comparison between these two time points, demonstrating suppression of infarct expansion and of LV dilatation in AdA-I MI mice, is not affected by survival bias.

Neovascularisation has a role in scar formation and scar tissue remodelling.[22] Increased neovascularisation was observed in the infarcts of AdA-I MI mice on day 28 after gene transfer. HDL is known to exert potent effects on the endothelium via enhanced endothelial survival,[23] endothelial cell migration[24] and EPC-mediated repair.[25,26] We did not observe enhanced incorporation of bone marrow-derived EPCs into the infarct zone. Nevertheless, increased EPC number and function following human *apo A-I* gene transfer[27] may have improved neovascularisation in a paracrine way by releasing angiogenic factors and proteases to stimulate sprouting of local vessels.[28]

Selective HDL-raising gene transfer significantly improved systolic and diastolic cardiac function after MI and led to a preservation of peripheral blood pressure compared with sham mice, in contrast to the lower blood pressure in control MI mice. In agreement, human *apo A-I* gene transfer has been shown to improve cardiac function in a rat model of diabetic cardiomyopathy.[13] Furthermore, HDL has also been demonstrated to increase cardiomyocyte contractility *ex vivo*.[13] Overall, the effect of human *apo A-I* gene transfer on cardiac function post MI may reflect both the effect of HDL on LV remodelling and direct potentiation of cardiomyocyte contractility by HDL.

Mortality was strongly reduced, and LV dilatation was significantly attenuated in control MI mice with prior irradiation and bone marrow transplantation compared with control MI mice without prior bone marrow transplantation. Notwithstanding this significantly milder phenotype, the effect of AdA-I transfer was confirmed. Infarct length was shorter, left ventricular dilatation was attenuated and LV function was improved in AdA-I MI mice compared with the control MI mice under conditions of prior bone marrow transplantation and irradiation. This independent set of experiments conducted in a different setting strongly corroborates our findings in animals without prior irradiation and bone marrow transplantation. The milder phenotype in bone marrow transplantation mice might be related to immune reset. CD4+ T helper cells and regulatory T cells have been demonstrated to have a role in infarct healing and myocardial remodelling.[29,30] Autologous bone marrow transplantation has been shown to reverse autoimmune arthritis in mice via induction of regulatory T cells.[31] In addition, clinical hematopoietic stem cell transplantation with either myeloablative or nonmyeloablative regimens

has been used for treatment of patients with severe autoimmune diseases.[32,33] Similarly, bone marrow transplantation in the current study may have altered T cell biology. Regulatory T cells may suppress inflammatory activity of monocytes by secreting inhibitory signals such as IL-10 and transforming growth factor-β, and through contact-mediated actions.[34]

In conclusion, this murine experimental study supports the hypothesis that HDL may be an important target for treatment of myocardial remodelling post MI, and for prevention and treatment of heart failure.

MATERIALS AND METHODS

Construction of E1E3E4-deleted adenoviral gene transfer vectors for hepatocyte restricted overexpression of human apo A-I
Construction of the E1E3E4-deleted adenoviral vector AdA-I has been described previously.[35] This vector contains the 1.2-kb DC172 promotor, consisting of an 890-bp human α_1-antitrypsin promoter and two copies of the 160-bp α_1-microglobulin enhancer, upstream of the genomic human *apo A-I* sequence and two copies of the hepatic control region-1. The E1E3E4-deleted control vector Adnull[36] does not contain an expression cassette. Vector production was performed as described previously.[37]

Animal experiments
All animal procedures were approved by the ethical committee for animal experimentation of the Catholic University of Leuven, Leuven, Belgium. Male C57BL/6 LDLr$^{-/-}$ mice, originally purchased from Jackson Laboratories (Bar Harbor, ME, USA), received a hypercholesterolemic diet containing 0.2% (w/w) cholesterol and 10% (v/w) coconut oil *ad libitum* starting from the age of 12 weeks. Gene transfer in C57BL/6 LDLr$^{-/-}$ mice was performed 3 weeks after the start of the hypercholesterolemic diet by tail vein injection of 5×10^{10} adenoviral particles of AdA-I. This dose was chosen based on a prior study on the effect of this vector on HDL levels and on atherosclerosis in C57BL/6 LDLr$^{-/-}$ mice.[38] Control mice were injected with the same dose of the control vector Adnull or with saline. As no differences were observed between the Adnull and saline-injected mice with regard to different end points, data of both the control groups were consistently pooled. The experimental diet was maintained throughout the entire duration of the experiments.

Two weeks after gene transfer or saline injection, MI was induced by permanent ligation of the LAD, as described.[39] In selected experiments, C57BL/6 LDLr$^{-/-}$ mice were lethally irradiated with 9.5 Gy at the age of 8 weeks. Transplantation of 8×10^6 bone marrow cells obtained from male C57BL/6 β-actin GFP-transgenic mice was performed via tail vein injection 24 h after irradiation. Feeding of the hypercholesterolemic diet was started 4 weeks after bone marrow transplantation. Gene transfer and MI were performed in chimeric mice at the age of 15 and 17 weeks, respectively.

In vivo hemodynamic measurements
Invasive hemodynamic measurements were performed 28 days after MI, following anaesthesia induced by intraperitoneal administration of 1.4 g kg^{-1} urethane (Sigma, Steinheim, Germany). Measurements were performed with a 1.1 French Millar pressure catheter (SPR-67/NR; Millar instruments, Houston, TX, USA), as described before.[39] Data were registered with Powerlab Bridge Amplifier and Chart Software (sampling rate 2000 Hz; Fysicon, Oss, the Netherlands).

Plasma lipoprotein and apo analysis
Mouse lipoproteins were separated by density gradient ultracentrifugation in a swing-out rotor.[40] Fractions were stored at −20 °C until analysis. Total cholesterol in plasma and lipoprotein fractions was determined with commercially available enzymes (Roche Diagnostics, Basel, Switzerland). Precipath L (Roche Diagnostics) was used as a standard. Human apo A-I levels in plasma were determined by sandwich ELISA.[41]

Area at risk and infarct size assessment 1 day after MI
Twenty-four hours after completion of the MI protocol, 2 ml of a blue tissue-marking dye (Polysciences, Warrington, PA, USA) was injected as a bolus into the aorta until most of the heart turned blue. Hearts were arrested in diastole by CdCl (100 µl; 0.1 N) and flushed with saline to wash out excess blue dye. After embedding the hearts in 5% low gelling temperature agarose (Sigma), 500-µm thick cross-sections were made

using a HM 650 V Vibration Microtome (MICROM International GmbH, Walldorf, Germany). The slices were then incubated in a 1.5% triphenyl tetrazolium chloride (Alfa Aesar, Ward Hill, MA, USA) solution in an isotonic phosphate buffer (pH 7.4) for 30 min at 37 °C. Images were made with a SteREO Lumar V.12 microscope (Zeiss, Zaventem, Belgium) and the areas of infarcted tissue, the non-infarcted area at risk, and the LV wall area were determined using Image J software (Wayne Rasband, National Institutes of Health, Bethesda, MD, USA).

Tissue preparation for histological and morphometric analysis

Mice were perfused via the abdominal aorta with phosphate-buffered saline and hearts were arrested in diastole by CdCl (100 μl; 0.1 N), followed by perfusion fixation with 1% paraformaldehyde in phosphate-buffered saline. Hearts and lungs were dissected and weighed. Hearts were post fixated overnight in 1% paraformaldehyde, embedded in paraffin and 6-μm thick cross-sections at 130-μm spaced intervals were made, extending from the apex to the basal part of the left ventricle.

Morphometric analysis of infarct expansion and LV remodelling

Infarct expansion and LV remodelling were assessed by morphometric analysis on mosaic images of Sirius Red-stained heart cross-sections using Axiovision 4.6 software (Zeiss). Longitudinal comparisons of parameters were based on data obtained on day 0 or on days 3, 14 or 28 after MI. Midline infarct length was defined as the midline length of infarct that included >50% of the whole thickness of the myocardial wall. Whole LV area (μm^2), LV cavity area (μm^2), LV remote muscle area (μm^2; including the septum), septal wall thickness (μm) and infarct area (μm^2) were analysed. Infarct wall thickness (μm) was measured at equidistant points over the infarct area perpendicular to the infarcted wall. All geometric measurements were computed in a blinded fashion from representative tissue sections of four separate regions, and the average value was used to represent that animal for statistical purposes.

Analysis of collagen deposition

To measure collagen content in the infarct zone and in the interstitium, Sirius Red staining was performed, as previously described by Junqueira et al.[42] Sirius Red polarisation microscopy on a Leica DM RBE microscope (Leica Microsystems, Wetzlar, Germany) with KS300 software (Zeiss) was used to quantify thick tightly packed mature collagen fibres as orange–red birefringent, and loosely packed less crosslinked and immature collagen fibres as yellow–green birefringent. Collagen-positive area was normalised to infarct area or LV remote area and was expressed as percentage. Two midventricular sections were studied per animal.

Immunohistochemistry

Cardiomyocyte hypertrophy was analysed on paraffin sections stained with rabbit anti-mouse laminin (Sigma; 1/50) by measuring the cardiomyocyte cross-sectional area (μm^2) of at least 200 randomly selected cardiomyocytes in the non-infarcted LV myocardium. Capillary density in the infarct area and in the non-infarcted myocardium was determined on CD31-stained sections using rat anti-mouse CD31 antibodies (BD Biosciences, Erembodegem, Belgium; 1/500). Two midventricular cross-sections were analysed per mouse.

To evaluate EPC incorporation in the infarct area, heart sections from bone marrow transplantation mice were immunohistochemically double stained with rabbit anti-mouse GFP (Molecular Probes, Carlsbad, CA, USA; 1/200) and rat anti-mouse CD31 (BD Biosciences; 1/500) antibodies. Nuclei were visualised with 4′,6-diamidino-2-phenylindole (Invitrogen, Carlsbad, CA, USA). Only GFP CD31 double-positive cells that colocalized with a 4′,6-diamidino-2-phenylindole signal were considered as bone marrow-derived endothelial cells. Data are expressed as the number of GFP$^+$ CD31$^+$ capillaries per mm^2 of cross-sectional area or as percentage of the total number of CD31$^+$ capillaries.

Quantitative reverse transcriptase polymerase chain reaction (qRT-PCR) analysis

Three days after MI, hearts were dissected, briefly rinsed with saline buffer, snap-frozen and stored at −80 °C until use. RNA was extracted from infarcted LV myocardium using TRIzol reagent (Invitrogen) and the Purelink RNA Mini Kit (Invitrogen). On-column DNase treatment was performed using Purelink DNase (Invitrogen), according to the manufacturer's protocol. Total RNA (1 μg) was reverse transcribed using the QuantiTect Reverse Transcription kit (Qiagen, Hamburg, Germany). qRT-PCR was performed on a 7500 FAST real-time PCR system (Applied Biosystems, Carlsbad, CA, USA) using the TaqMan Fast Universal PCR Master Mix (Applied Biosystems), and a premade mix containing primers and MGB probes (Taqman gene expression assay, Applied Biosystems; see Supplementary Table 3 for details) to quantify *IL1-β, IL-10, transforming growth factor β1, collagen type I α1* and *collagen type III α1* complementary cDNA levels (n = 8 per group). The *Gapdh* housekeeping gene was used as endogenous control. Data analysis was performed using $\Delta\Delta C_t$-based fold-change calculations.

Statistical analysis

All data are expressed as means ± s.e.m. Parameters between three groups were compared by one-way analysis of variance, followed by Tukey multiple comparison post-test using GraphPad Instat (GraphPad Software, San Diego, CA, USA). When indicated, a logarithmic transformation or a square root transformation or a non-parametric test was performed. Parameters between two groups were compared using Student's t-test. When indicated, a logarithmic transformation, a square root transformation or a non-parametric Mann–Whitney test was performed. The assumption of Gaussian distribution was tested using the method Kolmogorov and Smirnov. Kaplan–Meier survival curves were analysed by log-rank test using Prism4 (GraphPad Software). A two-sided P-value of <0.05 was considered statistically significant.

CONFLICT OF INTEREST

The authors declare no conflict of interest.

REFERENCES

1 Gordon DJ, Probstfield JL, Garrison RJ, Neaton JD, Castelli WP, Knoke JD et al. High-density lipoprotein cholesterol and cardiovascular disease. Four prospective American studies. Circulation 1989; 79: 8–15.

2 Su YR, Ishiguro H, Major AS, Dove DE, Zhang W, Hasty AH et al. Macrophage apolipoprotein A-I expression protects against atherosclerosis in ApoE-deficient mice and up-regulates ABC transporters. Mol Ther 2003; 8: 576–583.

3 Rader DJ. Molecular regulation of HDL metabolism and function: implications for novel therapies. J Clin Invest 2006; 116: 3090–3100.

4 Kopfler WP, Willard M, Betz T, Willard JE, Gerard RD, Meidell RS. Adenovirus-mediated transfer of a gene encoding human apolipoprotein A-I into normal mice increases circulating high-density lipoprotein cholesterol. Circulation 1994; 90: 1319–1327.

5 Belalcazar LM, Merched A, Carr B, Oka K, Chen KH, Pastore L et al. Long-term stable expression of human apolipoprotein A-I mediated by helper-dependent adenovirus gene transfer inhibits atherosclerosis progression and remodels atherosclerotic plaques in a mouse model of familial hypercholesterolemia. Circulation 2003; 107: 2726–2732.

6 Van Craeyveld E, Gordts S, Jacobs F, De Geest B. Gene therapy to improve high-density lipoprotein metabolism and function. Curr Pharm Des 2010; 16: 1531–1544.

7 Wang TD, Wu CC, Chen WJ, Lee CM, Chen MF, Liau CS et al. Dyslipidemias have a detrimental effect on left ventricular systolic function in patients with a first acute myocardial infarction. Am J Cardiol 1998; 81: 531–537.

8 Kempen HJ, van Gent CM, Buytenhek R, Buis B. Association of cholesterol concentrations in low-density lipoprotein, high-density lipoprotein, and high-density lipoprotein subfractions, and of apolipoproteins AI and AII, with coronary stenosis and left ventricular function. J Lab Clin Med 1987; 109: 19–26.

9 Velagaleti RS, Massaro J, Vasan RS, Robins SJ, Kannel WB, Levy D. Relations of lipid concentrations to heart failure incidence: the Framingham Heart Study. Circulation 2009; 120: 2345–2351.

10 Mehra MR, Uber PA, Lavie CJ, Milani RV, Park MH, Ventura HO. High-density lipoprotein cholesterol levels and prognosis in advanced heart failure. J Heart Lung Transplant 2009; 28: 876–880.

11 Iwaoka M, Obata JE, Abe M, Nakamura T, Kitta Y, Kodama Y et al. Association of low serum levels of apolipoprotein A-I with adverse outcomes in patients with nonischemic heart failure. *J Card Fail* 2007; **13**: 247–253.

12 Frias MA, James RW, Gerber-Wicht C, Lang U. Native and reconstituted HDL activate Stat3 in ventricular cardiomyocytes via ERK1/2: role of sphingosine-1-phosphate. *Cardiovasc Res* 2009; **82**: 313–323.

13 Van Linthout S, Spillmann F, Riad A, Trimpert C, Lievens J, Meloni M et al. Human apolipoprotein A-I gene transfer reduces the development of experimental diabetic cardiomyopathy. *Circulation* 2008; **117**: 1563–1573.

14 Theilmeier G, Schmidt C, Herrmann J, Keul P, Schafers M, Herrgott I et al. High-density lipoproteins and their constituent, sphingosine-1-phosphate, directly protect the heart against ischaemia/reperfusion injury *in vivo* via the S1P3 lysophospholipid receptor. *Circulation* 2006; **114**: 1403–1409.

15 Erlebacher JA, Weiss JL, Weisfeldt ML, Bulkley BH. Early dilation of the infarcted segment in acute transmural myocardial infarction: role of infarct expansion in acute left ventricular enlargement. *J Am Coll Cardiol* 1984; **4**: 201–208.

16 Eaton LW, Weiss JL, Bulkley BH, Garrison JB, Weisfeldt ML. Regional cardiac dilatation after acute myocardial infarction: recognition by two-dimensional echocardiography. *N Engl J Med* 1979; **300**: 57–62.

17 Erlebacher JA, Weiss JL, Eaton LW, Kallman C, Weisfeldt ML, Bulkley BH. Late effects of acute infarct dilation on heart size: a two dimensional echocardiographic study. *Am J Cardiol* 1982; **49**: 1120–1126.

18 Schuster EH, Bulkley BH. Expansion of transmural myocardial infarction: a pathophysiologic factor in cardiac rupture. *Circulation* 1979; **60**: 1532–1538.

19 Jugdutt BI, Michorowski BL. Role of infarct expansion in rupture of the ventricular septum after acute myocardial infarction: a two-dimensional echocardiographic study. *Clin Cardiol* 1987; **10**: 641–652.

20 Gao XM, Xu Q, Kiriazis H, Dart AM, Du XJ. Mouse model of post-infarct ventricular rupture: time course, strain- and gender-dependency, tensile strength, and histopathology. *Cardiovasc Res* 2005; **65**: 469–477.

21 Smythies LE, White CR, Maheshwari A, Palgunachari MN, Anantharamaiah GM, Chaddha M et al. Apolipoprotein A-I mimetic 4F alters the function of human monocyte-derived macrophages. *Am J Physiol Cell Physiol* 2010; **298**: C1538–C1548.

22 Wang B, Ansari R, Sun Y, Postlethwaite AE, Weber KT, Kiani MF. The scar neovasculature after myocardial infarction in rats. *Am J Physiol Heart Circ Physiol* 2005; **289**: H108–H113.

23 Nofer JR, Levkau B, Wolinska I, Junker R, Fobker M, von Eckardstein A et al. Suppression of endothelial cell apoptosis by high density lipoproteins (HDL) and HDL-associated lysosphingolipids. *J Biol Chem* 2001; **276**: 34480–34485.

24 Seetharam D, Mineo C, Gormley AK, Gibson LL, Vongpatanasin W, Chambliss KL et al. High-density lipoprotein promotes endothelial cell migration and reendothelialization via scavenger receptor-B type I. *Circ Res* 2006; **98**: 63–72.

25 Feng Y, Jacobs F, Van Craeyveld E, Brunaud C, Snoeys J, Tjwa M et al. Human ApoA-I transfer attenuates transplant arteriosclerosis via enhanced incorporation of bone marrow-derived endothelial progenitor cells. *Arterioscler Thromb Vasc Biol* 2008; **28**: 278–283.

26 Feng Y, van Eck M, Van Craeyveld E, Jacobs F, Carlier V, Van Linthout S et al. Critical role of scavenger receptor-BI-expressing bone marrow-derived endothelial progenitor cells in the attenuation of allograft vasculopathy after human apo A-I transfer. *Blood* 2009; **113**: 755–764.

27 Gordts SC, Van Craeyveld E, Muthuramu I, Singh N, Jacobs F, De Geest B. Lipid lowering and HDL raising gene transfer increase endothelial progenitor cells, enhance myocardial vascularity, and improve diastolic function. *PLoS One* 2012; **7**: e46849.

28 Rehman J, Li J, Orschell CM, March KL. Peripheral blood "endothelial progenitor cells" are derived from monocyte/macrophages and secrete angiogenic growth factors. *Circulation* 2003; **107**: 1164–1169.

29 Hofmann U, Beyersdorf N, Weirather J, Podolskaya A, Bauersachs J, Ertl G et al. Activation of CD4 + T lymphocytes improves wound healing and survival after experimental myocardial infarction in mice. *Circulation* 2012; **125**: 1652–1663.

30 Matsumoto K, Ogawa M, Suzuki J, Hirata Y, Nagai R, Isobe M. Regulatory T lymphocytes attenuate myocardial infarction-induced ventricular remodeling in mice. *Int Heart J* 2011; **52**: 382–387.

31 Roord ST, de Jager W, Boon L, Wulffraat N, Martens A, Prakken B et al. Autologous bone marrow transplantation in autoimmune arthritis restores immune homeostasis through CD4 + CD25 + Foxp3 + regulatory T cells. *Blood* 2008; **111**: 5233–5241.

32 Burt RK, Marmont A, Oyama Y, Slavin S, Arnold R, Hiepe F et al. Randomized controlled trials of autologous hematopoietic stem cell transplantation for autoimmune diseases: the evolution from myeloablative to lymphoablative transplant regimens. *Arthritis Rheum* 2006; **54**: 3750–3760.

33 Burt RK, Loh Y, Pearce W, Beohar N, Barr WG, Craig R et al. Clinical applications of blood-derived and marrow-derived stem cells for nonmalignant diseases. *JAMA* 2008; **299**: 925–936.

34 Frangogiannis NG. Regulation of the inflammatory response in cardiac repair. *Circ Res* 2012; **110**: 159–173.

35 Jacobs F, Snoeys J, Feng Y, Van Craeyveld E, Lievens J, Armentano D et al. Direct comparison of hepatocyte-specific expression cassettes following adenoviral and nonviral hydrodynamic gene transfer. *Gene Ther* 2008; **15**: 594–603.

36 Van Linthout S, Lusky M, Collen D, De Geest B. Persistent hepatic expression of human apo A-I after transfer with a helper-virus independent adenoviral vector. *Gene Ther* 2002; **9**: 1520–1528.

37 Snoeys J, Mertens G, Lievens J, van Berkel T, Collen D, Biessen EA et al. Lipid emulsions potently increase transgene expression in hepatocytes after adenoviral transfer. *Mol Ther* 2006; **13**: 98–107.

38 Van Craeyveld E, Gordts SC, Nefyodova E, Jacobs F, De Geest B. Regression and stabilization of advanced murine atherosclerotic lesions: a comparison of LDL lowering and HDL raising gene transfer strategies. *J Mol Med* 2011; **89**: 555–567.

39 Van Craeyveld E, Jacobs F, Gordts SC, De Geest B. Low-density lipoprotein receptor gene transfer in hypercholesterolemic mice improves cardiac function after myocardial infarction. *Gene Ther* 2012; **19**: 860–871.

40 Jacobs F, Van Craeyveld E, Feng Y, Snoeys J, De Geest B. Adenoviral low density lipoprotein receptor attenuates progression of atherosclerosis and decreases tissue cholesterol levels in a murine model of familial hypercholesterolemia. *Atherosclerosis* 2008; **201**: 289–297.

41 Van Linthout S, Collen D, De Geest B. Effect of promoters and enhancers on expression, transgene DNA persistence, and hepatotoxicity after adenoviral gene transfer of human apolipoprotein A-I. *Hum Gene Ther* 2002; **13**: 829–840.

42 Junqueira LC, Bignolas G, Brentani RR. Picrosirius staining plus polarisation microscopy, a specific method for collagen detection in tissue sections. *Histochem J* 1979; **11**: 447–455.

Supplementary Information accompanies this paper on Gene Therapy website (http://www.nature.com/gt)